**SHORT COMMUNICATION**

# Iron-Gallium and Cobalt-Gallium Tetraphosphido Complexes

Christoph G. P. Ziegler,[a] Felix Hennersdorf,[b] Jan J. Weigand,*[b] and Robert Wolf*[a]

*Dedicated to Professor Manfred Scheer on the Occasion of his 65th Birthday*

**Abstract**. The synthesis and characterization of two heterobimetallic complexes [K([18]crown-6){($\eta^4$-C$_{14}$H$_{10}$)Fe($\mu$-$\eta^4$:$\eta^2$-P$_4$)Ga(nacnac)}] (**1**) (C$_{14}$H$_{10}$ = anthracene) and [K(dme)$_2${($\eta^4$-C$_{14}$H$_{10}$)Co($\mu$-$\eta^4$:$\eta^2$-P$_4$)Ga(nacnac)}] (**2**) with strongly reduced P$_4$ units is reported. Compounds **1** and **2** are prepared by reaction of the gallium(III) complex [(nacnac)Ga($\eta^2$-P$_4$)] (nacnac = CH[CMeN(2,6-$i$Pr$_2$C$_6$H$_3$)]$_2$) with bis(anthracene)ferrate(1–) and -cobaltate(1–) salts. The molecular structures of **1** and **2** were determined by X-ray crystallography and feature a P$_4$ chain which binds to the transition metal atom via all four P atoms and to the gallium atom via the terminal P atoms. Multinuclear NMR studies on **2** suggest that the molecular structure is preserved in solution.

## Introduction

Since the discovery of the first transition metal complex of white phosphorus (P$_4$) by *Ginsberg* and *Lindsell* in 1970,[1] an extensive coordination chemistry has emerged for the P$_4$ molecule.[2,3] In numerous cases, the use of low-oxidation state metal complexes leads to formation of coordinated P$_n$ units with two to six P atoms ($n$ = 2–6).[2] Thereby, the size of the phosphorus framework is mainly dictated by the electronic requirements of the metal atom. While formally anionic, these P$_n$ units are typically not very reactive, although selected reports in the literature show that functionalizations of transition metal polyphosphides are feasible with electrophiles[3f,4] and, as shown by more recent literature, with nucleophiles.[3f,5]

The use of two electronically distinct metal atoms can generate strongly reduced P$_n$ fragments. However, such heterodinuclear complexes are relatively scarce.[6] Some relevant examples are shown in Figure 1. [{Cp*Co}{Cp′′(CO)Ta}($\mu$-$\eta^{2:2}$-P$_2$)$_2$] (**A**, Cp* = C$_5$Me$_5$, Cp′′ = C$_5$H$_3${1,3-$t$Bu$_2$}) was synthesized by *Scherer* and co-workers by reaction of [Cp′′(CO)$_2$Ta($\eta^4$-P$_4$)] with [Cp*Co($\eta^2$-C$_2$H$_4$)$_2$],[7] while the related complex [{Cp*Fe}{Cp′′Ta}($\mu$-$\eta^{4:3}$-P$_5$)] (**B**) is formed by cothermolysis of two sandwich compounds [Cp*Fe($\eta^5$-P$_5$)] and [Cp''Ta(CO)$_4$].[8] *Peruzzini* and co-workers described the insertion of platinum(0) complexes into polyphosphido ligands.[9]

Among other examples, such reactions resulted in complexes **C** and **D** shown in Figure 1. *Akbayeva* reported insertions into a P–P bond of $\eta^1$-P$_4$ complexes of ruthenium(II) and iron(II).[10]
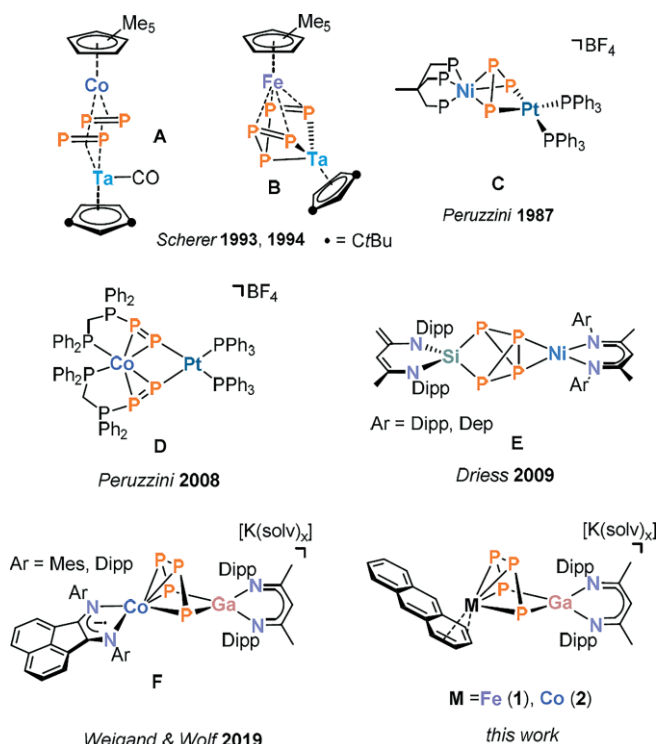


**Figure 1.** Selected examples of heterodinuclear transition metal tetraphosphido complexes.

Particularly relevant to the work described in this manuscript is a report by *Driess* and co-workers on heterodinuclear compounds of type **E**, which were synthesized from the silylene-activated P$_4$ ligand [(nacnac′)Si($\eta^2$-P$_4$)] (nacnac′ = CH[(C=CH$_2$)CMe][N(2,6-$i$Pr$_2$C$_6$H$_3$)]$_2$) and the nickel(I) species [({nacnac}Ni)$_2$·toluene] (nacnac = CH[CMeN(2,6-$i$Pr$_2$C$_6$H$_3$)]$_2$) and [({nacnac′′}Ni)$_2$· toluene] (nacnac′′ = CH[CMeN(2,6-Et$_2$C$_6$H$_3$)]$_2$).[11] These

* Prof. Dr. R. Wolf
  E-Mail: robert.wolf@ur.de
* Prof. Dr. J. J. Weigand
  E-Mail: jan.weigand@tu-dresden.de
[a] Institute of Inorganic Chemistry,
  University of Regensburg
  93040 Regensburg, Germany
[b] Faculty of Chemistry and Food Chemistry
  TU Dresden
  01062 Dresden, Germany

complexes feature an $[Si(\mu,\eta^{2:2}-P_4)Ni]$ core, where the $[(nacnac')Si(\eta^2-P_4)]$ ligand is side-on coordinated to a tetrahedral nickel(I) center. Significantly, a reductive P–P bond cleavage does not occur in this case.

We recently reported the synthesis of a related cobalt-gallium compound $[K(dme)_2\{(^{Mes}BIAN)Co(\mu-\eta^4:\eta^2-P_4)Ga(nacnac)\}]$ (**F**) containing the α-diimine ligand bis(mesitylimino)acenaphthenediimine ($^{Mes}BIAN$).[4d] Complex **F** is formed by reaction of $[K(Et_2O)\{(^{Mes}BIAN)Co(\eta^4-1,5-cod)\}]$[12] and the previously reported gallium tetraphosphido complex $[(nacnac)Ga(\eta^2-P_4)]$. The latter compound is readily accessible by reaction of $(nacnac)Ga^I$ with $P_4$.[13,14] In contrast to the structures of the aforementioned Ni compounds **E**, a highly reduced *catena*-$P_4^{4-}$ unit resulting from the oxidative addition of a P–P bond to cobalt is observed in the structure of complex **F**. Reactions with chlorophosphanes $R_2PCl$ and $RPCl_2$ afford pentacyclic *cyclo*-$P_5R_2$ ligands. Such a route thus offers the possibility to prepare new organofunctionalized polyphosphorus ligands in the coordination sphere of transition metal atoms.

Building on this initial work, we subsequently investigated whether the range of accessible heterobimetallic phosphorus compounds can be expanded by using related transition metalates. Herein, we describe the synthesis and structural characterization of $[K([18]crown-6)\{(\eta^4-C_{14}H_{10})Fe(\mu-\eta^4:\eta^2-P_4)Ga(nacnac)\}]$ (**1**) and $[K(dme)_2\{(\eta^4-C_{14}H_{10})Co(\mu-\eta^4:\eta^2-P_4)Ga(nacnac)\}]$ (**2**). These compounds show a similar $M(\mu-P_4)Ga$ motif as compound **F**, but feature a distinct ancillary ligand at the transition metal center.

## Results and Discussion

Expanding on the initial synthesis of **F** from $[K(Et_2O)\{(BIAN)Co(\eta^4-1,5-cod)\}]$[12] and $[(nacnac)Ga(\eta^2-P_4)]$,[13,14] similar reactions of bis(anthracene) complexes $[K([18]crown-6)(thf)_2][Fe(\eta^4-C_{14}H_{10})_2]$[15,16] and $[K(dme)_2][Co(\eta^4-C_{14}H_{10})_2]$[16,17] were examined according to Scheme 1. Such complexes are useful sources of "naked" $Fe^-$ and $Co^-$ anions due to the presence of labile anthracene ligands.[15–18]
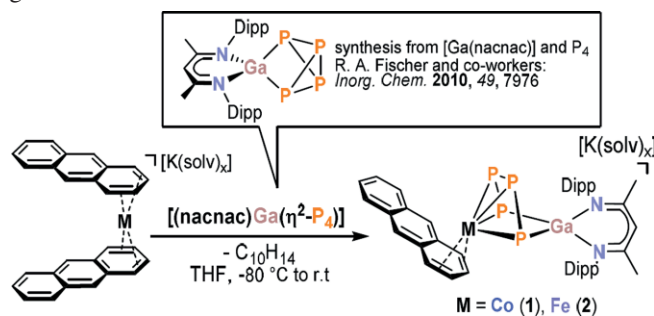


**Scheme 1.** Synthesis of **1** and **2**; reagents and conditions for **1**: $[K([18]crown-6)\{(\eta^4-C_{14}H_{10})Fe(\mu-\eta^4:\eta^2-P_4)Ga(nacnac)\}]$, for **2**: $[K(dme)_2\{(\eta^4-C_{14}H_{10})Co(\mu-\eta^4:\eta^2-P_4)Ga(nacnac)\}]$.

Slow addition of a yellow solution of $[(nacnac)Ga(\eta^2-P_4)]$ (one equiv.) to a cooled rust-colored solution of $[K([18]crown-6)(thf)_2][Fe(\eta^4-C_{14}H_{10})_2]$ affords a brownish-yellow solution. After work-up, dark crystals of **1** suitable for X-ray diffraction analysis can be obtained by slow diffusion of *n*-hexane into a concentrated DME solution of the crude product. Solid **1** is readily soluble in polar coordinating solvents such as DME and THF, and it is highly sensitive toward oxygen and moisture. Unfortunately, all attempts to isolate **1** as a pure compound were unsuccessful until now. Resonances of residual free anthracene are found in $^1H$ NMR spectra, while the C, H, N combustion analysis results gave variable results, which strongly deviated from the values expected for pure **1**. Nevertheless, the molecular structure of **1** was confirmed by single-crystal diffraction (XRD) analysis.

Complex **1** crystallizes in space group $P\bar{1}$ with two formula units per cell. The molecular structure is depicted in Figure 2. An ion-separated structure is observed where the potassium cation is coordinatively saturated by one molecule [18]crown-6 and one DME molecule. The anion shows a bridging $P_4$ chain that binds to the iron center with all four P atoms, while only the terminal P atoms coordinate the gallium atom. As a result of the coordination by two P atoms and a nacnac ligand, the gallium atom adopts a nearly ideal tetrahedral arrangement with a twist angle of 87.57°. The P–P bond lengths are all shorter than typical P–P single bonds.[25] Notably, the terminal P–P bonds [P1–P2 2.1166(6) Å and P3–P4 2.1131(7) Å] are significantly shorter than the internal P–P bond [P2–P3 2.1801(7) Å], whereas the distance between the terminal P atoms [P1–P4 3.5473(6) Å] is long. The dihedral angle (P1–P2–P3–P4 2.62°) shows that these bonds are nearly co-planar, while the P1–P2–P3 and P2–P3–P4 angles are almost identical [108.75(3)° and 108.93(3)°, respectively]. The anthracene ligand is $\eta^4$-coordinated to the iron center and shows the typical long-short-long pattern for the C–C bonds of transition-metal-coordinated anthracene molecules [C1–C2 1.4138(3) Å, C2–C3 1.409(3) Å, C3–C4 1.421(3) Å]. Based on Fe–C and C–C distances, the coordination mode of the anthracene ligand seems identical with that in the starting material $[K([18]crown-6)(thf)_2][Fe(\eta^4-C_{14}H_{10})_2]$.[15]

Cobalt complex **2** can be synthesized in a similar manner as **1** by adding a THF solution of $[(nacnac)Ga(\eta^2-P_4)]$ to a solution $[K(dme)_2][Co(\eta^4-C_{14}H_{10})_2]$ in THF. $^{31}P\{^1H\}$ NMR monitoring of the reaction revealed the selective formation of **2** as the sole P-containing species. As a result, this compound was isolated purely and is fully characterized. Released anthracene can be removed by extraction of the crude product with diethyl ether and *n*-hexane, and subsequent crystallization from DME/*n*-hexane affords **2** as thin, dark-violet plates, which were suitable for single-crystal XRD. Due to the elaborate work-up procedure, the yield of isolated compound is modest (22 %). Nevertheless, multinuclear NMR spectra and elemental analysis confirm the purity of the isolated compound.

Notably, the same compound **2** is formed as the major product even when an excess of $[(nacnac)Ga(\eta^2-P_4)]$ is employed in the reaction. Apparently, a substitution of the second anthracene ligand does not occur.

Complex **2** likewise crystallizes in space group $P\bar{1}$ with two formula units per cell, and the molecular structure is shown in
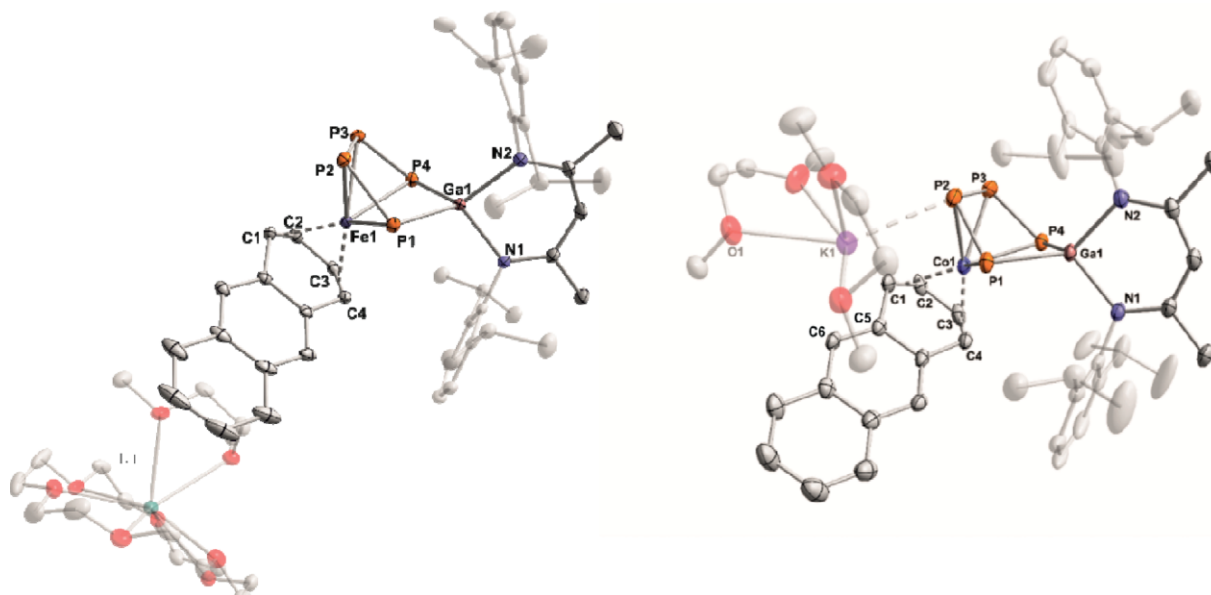
**Figure 2.** Solid-state molecular structures of **1** and **2**. Hydrogen atoms and some disordered parts are omitted for clarity; thermal ellipsoids are drawn at the 40% probability level. Selected bond lengths /Å and angles /° for **1**: P1–P2 2.1166(6), P2–P3 2.1801(7), P3–P4 2.1131(7), P1···P4 3.5473(6), Ga1–P1 2.3383(5), Ga1–P4 2.3307(5), Ga1–N1 2.018 (1), Ga1–N2 2.015(1), Fe1–P1 2.3879(5), Fe1–P2 2.3344(5), Fe1–P3 2.3368(7), Fe1–P4 2.3568(5), Fe1–C1 2.128(2), Fe1–C2 2.065(2), Fe1–C3 2.057(2), Fe1–C4 2.112(2), C1–C2 1.4138(3), C2–C3 1.409(3), C3–C4 1.421(3); P1–P2–P3 108.75(3), P2–P3–P4 108.94(3), P3–P4–Ga1 101.36(2), P4–Ga1–P1 98.89(2), Ga1–P1–P2 100.54(2), C4–Fe1–P1 97.07(5), C1–Fe1–P2 97.49(5), C2–Fe1–P3 101.14(5), C3–Fe1–P4 95.34(5); for **2**: P1–P2 2.1095(9), P2–P3 2.1825(9), P3–P4 2.1057(9), P1···P4 3.4509(8), Ga1–P1 2.3512(6), Ga1–P4 2.3297(6), Ga1–N1 1.993(2), Ga1–N2 2.008(2), Co1–P1 2.3635(7), Co1–P2 2.2922(7), Co1–P3 2.3368(7), Co1–P4 2.4108(7), Co1–C1 2.187(2), Co1–C2 2.026(2), Co1–C3 2.001(2), Co1–C4 2.82(2), C1–C2 1.4138(3), C2–C3 1.413(4), C3–C4 1.426(4), K1–P1 3.5646(9), K1–P2 3.2981(8); P1–P2–P3 109.13(3), P2–P3–P4 105.88(3), P3–P4–Ga1 101.3(3), P4–Ga1–P1 94.99(2), Ga1–P1–P2 98.41(3), C4–Co1–P1 113.18(7), C1–Co1–P2 126.01(8), C2–Co1–P3 121.78(8), C3–Co1–P4 104.08(7) K1–C5 3.370(2) Å, K1–C6 3.175(2).

Figure 2. In case of **2**, an ion-contact structure is observed [K1–P2 (3.298(1) Å], which is considerably shorter than the sum of the van der Waals radii (4.63 Å),[19] while it is slightly longer than the sum of the covalent radii (3.10 Å).[20] Furthermore, the potassium cation interacts with the anthracene ligand [K1–C5 3.370(2) Å, K1–C6 3.175(2) Å] and two DME molecules. The structure of the $Co(\mu-P_4)Ga$ core is nevertheless similar to that of **1**. The bridging $P_4$ unit is essentially in a syn conformation with a dihedral angle P1–P2–P3–P4 of 2.37°. The $P_4$ chain displays short terminal P–P bonds [P1–P2 2.1095(9) Å and P3–P4 2.1057(9) Å], whereas the internal P2–P3 bond [2.1825(9) Å] is closer to a single bond. The anthracene ligand coordinates to cobalt in an $\eta^4$-fashion. The C–C distances [C1–C2 1.4138(3) Å, C2–C3 1.413(4) Å, C3–C4 1.426(4) Å] indicate that there is considerable back-bonding between the metal atom and anthracene similar to the structures of **1** and other related anthracene metalates.[15,17]

In addition to complex **F**, several related structures with a $P_4$ fragment sandwiched between two metal atoms have been reported.[12,21] The most closely related compound appears to be $[(Cp^R Rh)(\mu-\eta^4:\eta^2-P_4)\{Rh(CO)Cp^R\}]$ $(Cp^R = \eta^5-C_5Me_4Et)$ reported by *Scherer* and co-workers.[22] In addition, it is noteworthy that *Roesky*, *Konchenko*, *Scheer*, and co-workers synthesized a trinuclear samarium-cobalt complex $[(Cp'''Co)_2(\mu_3-\eta^2:\eta^2:\eta^2-P_4)SmCp^*_2]$ $(Cp^* = \eta^5-C_5Me_5, Cp''' = \eta^5-1,2,4-tBu_3C_5H_2)$, which shows a similar structure motif.[23]

The $^1$H NMR spectrum of the isolated crystals of **2** dissolved in $[D_8]$THF displays five multiplets for coordinated anthracene with an integral ratio of 2:2:2:2:2. The chemical shifts of these resonances are in the range $\delta = 6.90$ ppm to 2.69 ppm, which is common for anthracene coordinated to a transition metal center.[17,24] The observed high-field shift of the anthracene signals is explained by π-donation from the metal atom to the π-acceptor ligand, which reduces the aromaticity of anthracene.[17] Two chemically distinct 2,6-diisoproplyphenyl groups are observed in accordance with the single-crystal X-ray structure, which are also discernible in the $^{13}$C{$^1$H} NMR spectrum. The $^{31}$P{$^1$H} NMR spectrum shows two higher order multiplets in a 1:1 ratio at $\delta = 89.2$ ppm and $\delta = -94.7$ ppm, which can be assigned to an AA′XX′ spin system shown in Figure 3. The AA′XX′ spin pattern observed is in line with a $C_2$ symmetrical $P_4$ moiety. The high-field shifted multiplet at $\delta = -94.7$ ppm can be tentatively assigned to the terminal phosphorus atoms bound to the gallium atom based on the larger line broadening and DFT calculations on the related compound **F**.[4d] Conversely, the signal at $\delta = 89.2$ ppm ($\tau_{1/2} = 10.64$ Hz) can be assigned to the internal phosphorus atoms. The $^1J_{AX}$ coupling constant is larger in magnitude than the $^1J_{AA'}$ coupling constant ($^1J_{AA'} - {}^1J_{AX} = 126.2$ Hz). This is in agreement with a putative partial double bond character of the terminal P–P bonds as suggested by the crystallographically obtained P–P distances (vide supra). The previously reported diimine complex **F** displays a similar AA′XX′ pattern in the $^{31}$P{$^1$H}

NMR spectrum with $^1J_{AX}$ = –450.5 Hz and $^1J_{AA'}$ = –380.2 Hz.[4d] Nevertheless, it is noteworthy that the magnitude of the $^1J_{AX}$ coupling constant of **1** is about 45 Hz higher than that of compound **F** ($^1J_{AX}$ = $^1J_{A'X'}$ = –450.5 Hz), while the $^1J_{AA'}$ constants are similar (**2**: $^1J_{AA'}$ = $^1J_{A'A}$ = –370.6 Hz; **C**: $^1J_{AA'}$ = $^1J_{A'A}$ = –380.5 Hz).[4d] The large difference of the $^1J_{AX}$ coupling constant might be caused by the shorter terminal P–P bonds in **2**. The $^2J_{PP}$ coupling constant is small ($^2J_{AX'}$ = $^2J_{A'X}$ = 4.9 Hz) and similar to those of **F** ($^2J_{AX'}$ = $^2J_{A'X}$ = 6.6 Hz).[4d] Remarkably, complex **1** shows a rather large $^3J_{PP}$ coupling constant ($^3J_{XX'}$ = $^3J_{X'X}$ = –52.2 Hz) compared to that determined in compound **F** ($^3J_{XX'}$ = $^3J_{X'X}$ = –7.2 Hz), which might be explained by the more co-planar alignment of the P-atoms of the P$_4$ chain of **2**. Overall, the multinuclear NMR spectra of **2** are in full agreement with the molecular structure observed in solid-state.
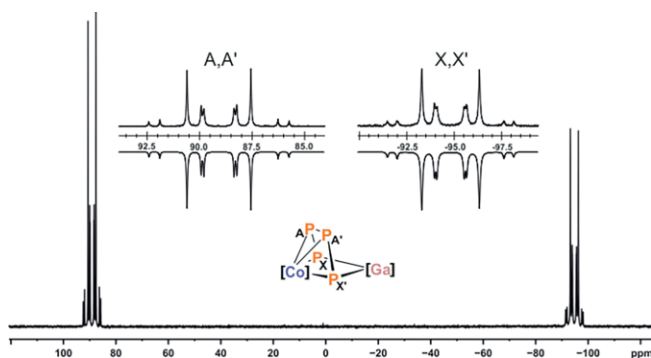


**Figure 3.** $^{31}$P{$^1$H} NMR spectrum of compound **2** (121.49 MHz, 300 K, [D$_8$]THF) with nuclei assigned to an AA'XX' spin system; insets: expanded spectrum (upwards) and simulated spectrum (downwards); δ(P$_{AA'}$) = 89.2 ppm, δ(P$_{XX'}$) = –94.7 ppm, $^1J_{AA'}$ = $^1J_{A'A}$ = –370.6, $^1J_{AX}$ = $^1J_{A'X'}$ = –496.8, $^2J_{AX'}$ = $^2J_{A'X}$ = 4.9, $^3J_{XX'}$ = $^3J_{X'X}$ = –52.2 Hz; [Co] = ($η^4$-C$_{14}$H$_{10}$)Co, [Ga] = (nacnac)Ga.

The UV/Vis spectrum of **2** was recorded in THF solution (see Figure S5, Supporting Information). The spectrum shows two very strong absorption bands in the UV region at 301 nm (ε = 42000 L·mol$^{-1}$·cm$^{-1}$) and 356 nm (ε = 39000 L·mol$^{-1}$·cm$^{-1}$), with the latter absorption tailing far into the visible region. The visible part shows a broad absorption at 524 nm. It is notable that the UV/Vis spectrum of **F** is similar in the UV region, while additional intense bands observed for **F** at 553 nm and 658 nm can be presumably assigned to charge transfer transitions involving the BIAN ligand.[4d]

In summary, heterodinuclear complexes with a strongly reduced P$_4$ unit were synthesized by oxidative P–P bond addition of [(nacnac)Ga($η^2$-P$_4$)] with low-valent ferrate(–I) and cobaltat(–I) anions. The molecular structures of the resulting complexes **1** and **2** feature an $η^4$:$η^2$-bridging P$_4$ chain between the transition metal atom and the gallium atom. Although bridging polyphosphide ligands are generally quite common in homodinuclear complexes,[2] this precise structural motif is rare, which underlines the flexible coordination behavior of polyphosphido ligands. In future work, substitution of the labile anthracene ligand in such complexes could enable the further derivatization of the P$_4$ ligand. In addition, it is noteworthy that polyphosphorus complexes containing the (nac-

nac)Ga moiety have recently emerged as promising platforms for the construction of extensive P$_n$ frameworks.[4d,14] Therefore, the complexes reported herein and related species might become a suitable starting point for further transformations leading to structurally novel species.

## Experimental Section

**General:** All manipulations were performed under an atmosphere of dry argon using standard Schlenk techniques or an MBraun UniLab glovebox. Solvents were dried and degassed with an MBraun SPS800 solvent-purification system. THF, diethyl ether, and toluene were stored over molecular sieves (3 Å). *n*-Hexane was stored over a potassium mirror. 1,2-dimethoxyethane (DME) was stirred over K/benzophenone, distilled and stored over molecular sieves (3 Å). Deuterated tetrahydrofurane was purchased from Sigma–Aldrich and used as received. The starting materials [(nacnac)Ga($η^2$-P$_4$)],[13] [K([18]crown-6)(thf)$_2$][Fe($η^4$-C$_{14}$H$_{10}$)$_2$],[15,16] and [K(dme)$_2$][Co($η^4$-C$_{14}$H$_{10}$)$_2$],[16,17] were prepared according to previously reported procedures.

**NMR Spectroscopy:** NMR spectra were recorded on Bruker Avance 300 and Avance 400 spectrometers at 300 K and internally referenced to residual solvent resonances (δ(TMS) = 0.00 ppm,$^1$H,$^{13}$C; δ(H$_3$PO$_4$) (85 %) = 0.00 ppm, $^{31}$P, externally). Chemical shifts (δ) are reported in ppm. Coupling constants (*J*) are reported in Hz. For compounds, which give rise to a higher order spin system in the $^{31}$P{$^1$H} NMR spectrum, the resolution enhanced $^{31}$P{$^1$H} NMR spectrum was transferred to the software gNMR, version 5.0, by Cherwell Scientific.[25] The full line shape iteration procedure of gNMR was applied to obtain the best match of the fitted to the experimental spectrum. $^1J$($^{31}$P$^{31}$P) coupling constants were set to negative values and all other signs of the coupling constants were obtained accordingly. The assignment of the $^{13}$C signals was deduced from the cross-peaks in 2D correlation experiments (HMBC, HSQC).

**Elemental Analysis:** Elemental analyses were determined by the analytical department of the University of Regensburg with a Micro Vario Cube (Elementar). UV/Vis spectra were recorded on an Ocean Optics Flame spectrometer.

**Single-crystal X-ray Diffraction:** Crystallographic data were recorded on an Oxford Diffraction Gemini R Ultra with Atlas S2 CCD detector for **1** and an Agilent GV1000 diffractometer with a Titan S2 CCD detector for **2**. In both cases, Cu-$K_α$ radiation (λ = 1.54184 Å) was used. Crystals were selected under mineral oil, mounted on micromount loops and quench-cooled using an Oxford Cryosystems open flow N$_2$ cooling device. Either semi-empirical multi-scan absorption corrections[26] or analytical ones[27] were applied to the data. Using Olex2,[28] the structures were solved with SHELXT[29] using intrinsic phasing and refined with SHELXL[30] using least-squares refinement on $F^2$. The hydrogen atoms were located in idealized positions and refined isotropically with a riding model.

Crystallographic data (excluding structure factors) for the structures in this paper have been deposited with the Cambridge Crystallographic Data Centre, CCDC, 12 Union Road, Cambridge CB21EZ, UK. Copies of the data can be obtained free of charge on quoting the depository numbers CCDC-1972352 for **1** and CCDC-1972351 for **2** (Fax: +44-1223-336-033; E-Mail: deposit@ccdc.cam.ac.uk, http://www.ccdc.cam.ac.uk).

**Crystallographic Data for 1:** C$_{66}$H$_{102}$FeGaKN$_2$O$_{10}$P$_4$ (*M* = 1372.04 g·mol$^{-1}$), triclinic, space group $P\bar{1}$ (no. 2), *a* = 12.8013(4) Å,

$b = 12.8477(3)$ Å, $c = 22.8788(6)$ Å, $\alpha = 95.470(2)°$, $\beta = 99.362(2)°$, $\gamma = 105.796(2)°$, $V = 3533.66(17)$ Å$^3$, $Z = 2$, $T = 123(1)$ K, $\mu$(Cu-$K_\alpha$) = 3.933 mm$^{-1}$, $D$(calcd) = 1.290 g·cm$^{-3}$, 51666 reflections measured ($7.23° \leq 2\Theta \leq 133.694°$), 12403 unique ($R_{int} = 0.0334$, $R_{sigma} = 0.0246$) which were used in all calculations. The final $R_1$ was 0.0314 [$I > 2\sigma(I)$], and $wR_2$ was 0.0816 (all data).

**Crystallographic Data for 2:** C$_{51}$H$_{71}$CoGaKN$_2$O$_4$P$_4$ ($M$ = 1067.72 g·mol$^{-1}$), triclinic, space group $P\bar{1}$ (no. 2), $a = 10.9891(2)$ Å, $b = 12.0239(2)$ Å, $c = 21.5532(3)$ Å, $\alpha = 90.3270(10)°$, $\beta = 92.4990(10)°$, $\gamma = 104.3790(10)°$, $V = 2755.63(8)$ Å$^3$, $Z = 2$, $T = 123.01(10)$ K, $\mu$(Cu-$K_\alpha$) = 5.059 mm$^{-1}$, $D$(calcd) = 1.287 g·cm$^{-3}$, 71275 reflections measured ($7.592° \leq 2\Theta \leq 147.664°$), 11035 unique ($R_{int} = 0.0509$, $R_{sigma} = 0.0286$) which were used in all calculations. The final $R_1$ was 0.0394 [$I > 2\sigma(I)$] and $wR_2$ was 0.1051 (all data).

**Synthesis of [K([18]crown-6){($\eta^4$-C$_{14}$H$_{10}$)Fe($\mu$-$\eta^4$:$\eta^2$-P$_4$)Ga(nacnac)}] (1):** A yellow solution of [(nacnac)Ga($\eta^2$-P$_4$)] (12 mg, 0.018 mmol, 1.0 equiv.) in THF (2 mL) was slowly added to a rust-colored solution of [K([18]crown-6)(thf)$_2$][Fe($\eta^4$-C$_{14}$H$_{10}$)$_2$] (15.7 mg, 0.018 mmol, 1 equiv.) in THF (2 mL). The reaction mixture was stirred for 24 h at room temperature. Volatiles were removed under reduced pressure and the residual brown solid was washed with 8 mL *n*-hexane. The crude product was dissolved in 4 mL DME and filtered through a Whatman glass filter (pore size: 0.1 μm). Crystals suitable for X-ray diffraction were obtained by diffusion of *n*-hexane into the concentrated filtrate of the crude product at room temperature. $^1$H NMR spectra of isolated samples of paramagnetic **1** show resonances of residual free anthracene. In addition, inconsistent and variable elemental analyses indicate the presence of large quantities of other unknown impurities. Unfortunately, all attempts to purify **1** by fractional crystallization were unsuccessful so far.

**Synthesis of [K(dme)$_2$){($\eta^4$-C$_{14}$H$_{10}$)Co($\mu$-$\eta^4$:$\eta^2$-P$_4$)Ga(nacnac)}] (2):** [K(dme)$_2$Co($\eta^4$-C$_{14}$H$_{10}$)$_2$] (199 mg, 0.315 mmol, 1.0 equiv.) was dissolved in THF (20 mL), resulting in a deep-violet solution, and a yellow solution of [(nacnac)Ga($\eta^2$-P$_4$)] (200 mg, 0.315 mmol, 1.0 equiv.) in 40 mL THF was slowly added at –80 °C. The reaction mixture was allowed to warm to room temperature while stirring. Volatiles were removed in vacuo and the remaining solid was washed with diethyl ether (20 mL) and *n*-hexane (40 mL). The brownish residue was redissolved in DME and filtered through a P4 glass frit. The dark red-brown filtrate was concentrated in vacuo and layered with *n*-hexane (35 mL). Pure [K(dme)$_2$){($\eta^4$-C$_{14}$H$_{10}$)Co($\mu$-$\eta^4$:$\eta^2$-P$_4$)Ga(nacnac)}] (**2**) was isolated as dark violet thin plates after storage at room temperature for five days. Based on $^1$H NMR spectroscopy and C,H,N analysis, **2** contains 1.9 molecules of DME per formula unit after drying under vacuum ($10^{-3}$ mbar) for several hours. Yield: 86 mg (22%). M.p. 178 °C (decomposition to black oil). **UV/Vis** (THF, $\lambda_{max}$ /nm, $\varepsilon_{max}$ /L·mol$^{-1}$·cm$^{-1}$): 301 (42000), 356 (39000), 524sh (8200). **$^1$H NMR** (400.13 MHz, 300 K, [D$_8$]THF): $\delta$ = 7.49 (br. m, 3 H, CH$_{Dipp}$), 6.99 (m, 1 H, CH$_{Dipp}$), 6.93 (m, 2 H, CH$_{Dipp}$), 6.90 (m, 2 H, CH$_{(anth)}$), 6.74 (m, 2 H,CH$_{(anth)}$), 5.84 (s, 2 H, CH$_{(anth)}$), 5.59 (m, 2 H, CH$_{(anth)}$), 4,82 (s, 1 H, CH$_{nacnac}$), 3.96 (sept, $^3J_{HH} = 6.8$ Hz, 2 H, C$H$(CH$_3$)$_{2(nacnac)}$), 3.44 (s, 7.6H DME), 3.27 (s, 11 H, DME), 2.88 [sept, $^3J_{HH} = 6.8$ Hz, 2 H, C$H$(CH$_3$)$_{2(nacnac)}$], 2.62 (m, 2 H, CH$_{(anth1,4)}$), 1.79 (s, 3 H, (s, 3 H, CH$_{3(nacnac)}$), 1.53 [d, $^3J_{HH} = 6.8$ Hz, 6 H, CH(C$H_3$)$_{2(nacnac)}$], 1.50 (s, 3 H, CH$_{3(nacnac)}$), 1.38 [d, $^3J_{HH} = 6.8$ Hz, 6 H, CH(C$H_3$)$_{2(nacnac)}$], 1.25 [d, $^3J_{HH} = 6.8$ Hz, 6 H, CH(C$H_3$)$_{2(nacnac)}$], 0.94 [d, $^3J_{HH} = 6.8$ Hz, 6 H, CH(C$H_3$)$_{2(nacnac)}$] ppm. **$^{13}$C{$^1$H} NMR** (100.61 MHz, 300 K, [D$_8$]THF): $\delta$ = 168.0 (NC$C$H$_3$CH$_{(nacnac)}$), 165.0 (NC$C$H$_3$CH$_{(nacnac)}$), 145.5 (C$_{(anth)}$), 145.1 (C$_{(Dipp)}$), 145.0 (C$_{(Dipp)}$), 144.1 (C$_{(Dipp)}$), 143.2 (C$_{(Dipp)}$), 133.3 (C$_{(anth)}$), 127.0 (C$_{(Dipp)}$), 126.2 (CH$_{(Dipp)}$), 125.8 (C$_{(anth)}$), 125.6 (CH$_{(Dipp)}$), 123.9 (CH$_{(Dipp)}$), 123.1 (C$_{(anth)}$), 113.5 (C$_{(anth)}$), 95.8

(CH$_{(nacnac)}$), 83.9 (C$_{(anth)}$), 72.6 (DME), 58.8 (DME), 56.4 (C$_{(anth)}$), 29.3 [CH(CH$_3$)$_{2(Dipp)}$], 28.7 [CH(CH$_3$)$_{2(Dipp)}$], 26.1 [CH(C$H_3$)$_{2(Dipp)}$], 25.9 [CH(C$H_3$)$_{2(Dipp)}$], 25.1 [CH(C$H_3$)$_{2(Dipp)}$], 24.6 (CH$_{3(Dipp)}$), 24.5 (CH$_{3(Dipp)}$) ppm. **$^{31}$P{$^1$H} NMR** (161.98 MHz, 300 K, [D$_8$]THF): (AA'XX') spin system $\delta$ = 89.2 (m, 2P$_P$), –94.7 (m, 2P$_{Ga}$) ppm; see Figure 3 for chemical shifts and coupling constants obtained by simulation. C$_{51}$H$_{71}$CoGaKN$_2$O$_4$P$_4$·(C$_4$H$_{10}$O$_2$)$_{1.9}$ (Mw = 1058.78 g·mol$^{-1}$): calcd. C 57.40, H 6.66, N 2.65%; found C 57.51, H 6.52, N 2.59%.

**Supporting Information** (see footnote on the first page of this article): Further details of the refinement and the crystallographic data of **1** and **2**.

## References

[1] a) A. P. Ginsberg, W. E. Lindsell, W. E. Silverthorn, *Trans. Acad. Sci. N. Y.* **1970**, 303; b) A. P. Ginsberg, W. E. Lindsell, *J. Am. Chem. Soc.* **1971**, 93, 2082–2084.

[2] a) M. Peruzzini, L. Gonsalvi, A. Romerosa, *Chem. Soc. Rev.* **2005**, 34, 1038–1047; b) M. Scheer, G. Balázs, A. Seitz, *Chem. Rev.* **2010**, 110, 4236–4256; c) M. Caporali, L. Gonsalvi, A. Rossin, M. Peruzzini, *Chem. Rev.* **2010**, 110, 4178–4235; d) B. M. Cossairt, N. A. Piro, C. C. Cummins, *Chem. Rev.* **2010**, 110, 4164–4177.

[3] Selected recent examples: a) S. Pelties, D. Herrmann, B. d. Bruin, F. Hartl, R. Wolf, *Chem. Commun.* **2014**, 50, 7014–7016; b) C. C. Mokhtarzadeh, A. L. Rheingold, J. S. Figueroa, *Dalton Trans.* **2016**, 45, 14561–14569; c) E. Mädl, G. Balázs, E. V. Peresypkina, M. Scheer, *Angew. Chem. Int. Ed.* 2016, 55, 7702–7707; *Angew. Chem.* **2016**, 128, 7833–7838; d) F. Dielmann, A. Timoshkin, M. Piesch, G. Balázs, M. Scheer, *Angew. Chem. Int. Ed.* 2017, 56, 1671–1675; *Angew. Chem.* **2017**, 129, 1693–1698; e) C. Chan, A. E. Carpenter, M. Gembicky, C. E. Moore, A. L. Rheingold, J. S. Figueroa, *Organometallics* **2019**, 38, 1436–1444; f) C. M. Hoidn, T. M. Maier, K. Trabitsch, J. J. Weigand, R. Wolf, *Angew. Chem. Int. Ed.* **2019**, 58; *Angew. Chem.* **2019**, 131, 19107–19112.

[4] a) G. Capozzi, L. Chiti, M. Di Vaira, M. Peruzzini, P. Stoppioni, *J. Chem. Soc., Chem. Commun.* **1986**, 1799–1800; b) B. M. Cossairt, M.-C. Diawara, C. C. Cummins, *Science* **2009**, 323, 602; c) A. E. Seitz, M. Eckhardt, A. Erlebach, E. V. Peresypkina, M. Sierka, M. Scheer, *J. Am. Chem. Soc.* **2016**, 138, 10433–10436; d) C. G. P. Ziegler, T. M. Maier, S. Pelties, C. Taube, F. Hennersdorf, A. W. Ehlers, J. J. Weigand, R. Wolf, *Chem. Sci.* **2019**, 110, 4178.

[5] a) P. Barbaro, M. Di Vaira, M. Peruzzini, S. Seniori Costantini, P. Stoppioni, *Chem. Eur. J.* **2007**, 13, 6682–6690; b) E. Mädl, M. V. Butovskii, G. Balázs, E. V. Peresypkina, A. V. Virovets, M. Seidl, M. Scheer, *Angew. Chem. Int. Ed.* 2014, 53, 7643–7646; *Angew. Chem.* **2014**, 126, 7774–7777; c) M. Piesch, S. Reichl, M. Seidl, G. Balázs, M. Scheer, *Angew. Chem. Int. Ed.* **2019**, 58, 16563–16568; *Angew. Chem.* **2019**, 131, 16716–16721.

[6] a) M. Di Vaira, P. Stoppioni, *Polyhedron* **1994**, 13, 3045–3051; b) O. J. Scherer, T. Mohr, G. Wolmershäuser, *J. Organomet. Chem.* **1997**, 529, 379–385; d) M. Caporali, M. Di Vaira, M. Per-

uzzini, S. Seniori Costantini, P. Stoppioni, F. Zanobini, *Eur. J. Inorg. Chem.* **2010**, *2010*, 152–158; d) V. Mirabello, M. Caporali, V. Gallo, L. Gonsalvi, A. Ienco, M. Latronico, P. Mastrorilli, M. Peruzzini, *Dalton Trans.* **2011**, *40*, 9668–9671; e) M. Piesch, F. Dielmann, S. Reichl, M. Scheer, *Chem. Eur. J.* **2020**, *26*, 1518–1524; f) M. Scheer, M. Piesch, C. Graßl, *Angew. Chem. Int. Ed.* **2020** DOI: 10.1002/anie.201916622; *Angew. Chem.* DOI: 10.1002/ange.201916622.

[7] O. J. Scherer, R. Winter, G. Wolmershäuser, *Z. Anorg. Allg. Chem.* **1993**, *619*, 827–835.

[8] M. Detzel, T. Mohr, O. J. Scherer, G. Wolmershäuser, *Angew. Chem. Int. Ed. Engl.* **1994**, *33*, 1110–1112; *Angew. Chem.* **1994**, *106*, 1142–1144.

[9] a) M. Di Vaira, P. Stoppioni, M. Peruzzini, *Polyhedron* **1987**, *6*, 351–382; b) M. Caporali, P. Barbaro, L. Gonsalvi, A. Ienco, D. Yakhvarov, M. Peruzzini, *Angew. Chem. Int. Ed.* **2008**, *47*, 3766–3768; *Angew. Chem.* **2008**, *120*, 3826–3828.

[10] D. N. Akbayeva, *Russ. J. Coord. Chem.* **2007**, *33*, 661–668.

[11] Y. Xiong, S. Yao, E. Bill, M. Driess, *Inorg. Chem.* **2009**, *48*, 7522–7524.

[12] S. Pelties, T. Maier, D. Herrmann, B. de Bruin, C. Rebreyend, S. Gärtner, I. G. Shenderovich, R. Wolf, *Chem. Eur. J.* **2017**, *23*, 6094–6102.

[13] G. Prabusankar, A. Doddi, C. Gemel, M. Winter, R. A. Fischer, *Inorg. Chem.* **2010**, *49*, 7976–7980.

[14] a) F. Hennersdorf, J. J. Weigand, *Angew. Chem. Int. Ed.* 2017, *56*, 7858–7862; *Angew. Chem.* **2017**, *129*, 7966–7970; b) F. Hennersdorf, J. Frötschel, J. J. Weigand, *J. Am. Chem. Soc.* **2017**, *139*, 14592–14604.

[15] W. W. Brennessel, R. E. Jilek, J. E. Ellis, *Angew. Chem. Int. Ed.* 2007, *46*, 6132–6136; *Angew. Chem.* **2007**, *119*, 6244–6248.

[16] W. W. Brennessel J. E. Ellis in *Inorganic Syntheses* (Ed.: P. P. Power), vol. 37, chapter 4.8., Wiley, pp. 76–84.

[17] a) W. W. Brennessel, J. V. G. Young, J. E. Ellis, *Angew. Chem. Int. Ed.* 2002, *41*, 1211–1215; *Angew. Chem.* **2002**, *114*, 1259–1263; b) W. W. Brennessel, J. E. Ellis, *Inorg. Chem.* **2012**, *51*, 9076–9094.

[18] a) J. E. Ellis, *Inorg. Chem.* **2006**, *45*, 3167–3186; b) R. Wolf, A. W. Ehlers, J. C. Slootweg, M. Lutz, D. Gudat, M. Hunger, A. L. Spek, K. Lammertsma, *Angew. Chem. Int. Ed.* 2008, *47*, 4584–4587; *Angew. Chem.* **2008**, *120*, 5660–5663; c) R. Wolf, J. C. Slootweg, A. W. Ehlers, F. Hartl, B. de Bruin, M. Lutz, A. L. Spek, K. Lammertsma, *Angew. Chem. Int. Ed.* 2009, *48*, 3104–3107; *Angew. Chem.* **2009**, *121*, 3150–3153; d) R. Wolf, N. Ghav-

tadze, K. Weber, E.-M. Schnöckelborg, B. d. Bruin, A. W. Ehlers, K. Lammertsma, *Dalton Trans.* **2010**, *39*, 1453–1456.

[19] P. Pyykkö, M. Atsumi, *Chem. Eur. J.* **2009**, *15*, 12770–12779.

[20] S. Alvarez, *Dalton Trans.* **2013**, *42*, 8617–8636.

[21] a) O. J. Scherer, G. Berg, G. Wolmershäuser, *Chem. Ber.* **1995**, *128*, 635–639; b) O. J. Scherer, S. Weigel, G. Wolmershäuser, *Chem. Eur. J.* **1998**, *4*, 1910–1916; c) V. A. Miluykov, O. G. Sinyashin, P. Lönnecke, E. Hey-Hawkins, *Mendeleev Commun.* **2003**, *13*, 212–213; d) W. W. Seidel, O. T. Summerscales, B. O. Patrick, M. D. Fryzuk, *Angew. Chem. Int. Ed.* 2008, *47*, 115–117; *Angew. Chem.* **2008**, *120*, 121–123; e) S. Yao, Y. Xiong, C. Milsmann, E. Bill, S. Pfirrmann, C. Limberg, M. Driess, *Chem. Eur. J.* **2010**, *16*, 436–439; f) C. Schwarzmaier, M. Bodensteiner, A. Y. Timoshkin, M. Scheer, *Angew. Chem. Int. Ed.* **2014**, *53*, 290–293; g) S. Yao, N. Lindenmaier, Y. Xiong, S. Inoue, T. Szilvási, M. Adelhardt, J. Sutter, K. Meyer, M. Driess, *Angew. Chem. Int. Ed.* 2015, *54*, 1250–1254; *Angew. Chem.* **2015**, *127*, 1266–1270; h) S. Yao, T. Szilvási, N. Lindenmaier, Y. Xiong, S. Inoue, M. Adelhardt, J. Sutter, K. Meyer, M. Driess, *Chem. Commun.* **2015**, *51*, 6153–6156; i) F. Spitzer, C. Graßl, G. Balázs, E. M. Zolnhofer, K. Meyer, M. Scheer, *Angew. Chem. Int. Ed.* 2016, *55*, 4340–4344; *Angew. Chem.* **2016**, *128*, 4412–4416; j) U. Chakraborty, J. Leitl, B. Mühldorf, M. Bodensteiner, S. Pelties, R. Wolf, *Dalton Trans.* **2018**, *47*, 3693–3697.

[22] O. J. Scherer, M. Swarowsky, H. Swarowsky, G. Wolmershäuser, *Angew. Chem. Int. Ed. Engl.* 1988, *27*, 694–695; *Angew. Chem.* **1988**, *100*, 738–739.

[23] T. Li, N. Arleth, M. T. Gamer, R. Köppe, T. Augenstein, F. Dielmann, M. Scheer, S. N. Konchenko, P. W. Roesky, *Inorg. Chem.* **2013**, *52*, 14231–14236.

[24] P. Büschelberger, D. Gärtner, E. Reyes-Rodriguez, F. Kreyenschmidt, K. Koszinowski, A. Jacobi von Wangelin, R. Wolf, *Chem. Eur. J.* **2017**, *23*, 3139–3151.

[25] P. H. M. Budzelaar, gNMR for Windows (5.0.6.0), NMR Simulation Programm 2006.

[26] a) SCALE3ABS, CrysAlisPro, Aglient Technologies Inc. Oxford, GB 2015; b) G. M. Sheldrick, SADABS, Bruker AXS, Madison, USA 2007.

[27] R. C. Clark, J. S. Reid, *Acta Crystallogr., Sect. A* **1995**, *51*, 887.

[28] O. V. Dolomanov, L. J. Bourhis, R. J. Gildea, J. A. K. Howard, H. Puschmann, *J. Appl. Crystallogr.* **2009**, *42*, 339–341.

[29] G. M. Sheldrick, *Acta Crystallogr., Sect. A* **2015**, *71*, 3.

[30] G. M. Sheldrick, *Acta Crystallogr., Sect. C* **2015**, *71*, 3.